IEEE Access
Multidisciplinary | Rapid Review | Open Access Journal

Received 5 January 2023, accepted 30 January 2023, date of publication 3 February 2023, date of current version 9 February 2023.

Digital Object Identifier 10.1109/ACCESS.2023.3242331

THEORY

An Amplitude-Phase Representation of the North-East-Down Kinematic Differential Equations

THOR I. FOSSEN, (Fellow, IEEE)
Department of Engineering Cybernetics, Norwegian University of Science and Technology, 7491 Trondheim, Norway
e-mail: thor.fossen@ntnu.no

ABSTRACT The overall goal of the paper is to derive a kinematic model for vehicle path-following systems, where the pitch and yaw angles (θ, ψ) together with the surge velocity u can be treated as control inputs. Then the outer control loop can be designed as a nonlinear path-following guidance law. At the same time, the inner control loops can be stabilized using commercial autopilot systems to control the pitch and yaw angles. The main result of the paper is a novel kinematic amplitude-phase representation of the North-East-Down (NED) positional rates, which can replace the classical Euler angle rotation matrix representation. The proposed kinematic model gives equivalent NED positional rates as the rotation matrix representation for all combinations of the Euler angles and the linear velocities. The main advantage of the kinematic amplitude-phase representation is the design of vehicle guidance laws using nonlinear control theory and Lyapunov stability analysis. Furthermore, it is shown that nonlinear guidance laws can be designed for path following and that the proposed methods guarantee that the origins are uniformly semiglobally exponentially stable (USGES). A case study of an unmanned surface vehicle (USV) demonstrates how a path-following control system can be designed using the amplitude-phase representation.

INDEX TERMS Aircraft, autonomous vehicles, guidance systems, kinematics, marine vehicles, mobile robot kinematics, underwater vehicles.

I. INTRODUCTION

Te purpose of this paper is to introduce a new kinematic model for the North-East-Down (NED) positional rates, which can be used to design intuitive and efficient control systems for path following and path tracking. The proposed amplitude-phase representation is an alternative to existing models for guidance-based path following in 3-D space parametrized by rotation matrices on SO(3), see [1]. The amplitude-phase representation of the NED kinematic differential equations uses the pitch and yaw angles (θ, ψ), and the surge velocity u as control inputs, see Figure 1. Pitch and yaw angle commands can be implemented using standard aircraft and marine craft autopilot systems, see [2] and [3], while a speed controller can stabilize the surge velocity. The autopilot systems are recognized as the inner control loops in Figure 1, while the path-following guidance laws represent the outer control loops. The structural properties of the kinematic amplitude-phase equations are exploited when designing the guidance laws [3]. Lyapunov stability analysis guarantees that the line-of-sight (LOS) guidance laws for path following will render the origin of the outer control loop uniformly semiglobally exponentially stable (USGES) [4].

A large number of authors has discussed proportional LOS guidance laws for path following using approximate amplitude-phase models where couplings to the roll motion are neglected; see [5], [6], [7], [8], [9], [10], [11], [12], [13], and [14]. The results in the paper generalize this to six degrees of freedom (DOFs) coupled motions.

The main result of the paper is a novel kinematic amplitude-phase representation of the NED positional rates, which can replace the classical Euler angle rotation matrix

The associate editor coordinating the review of this manuscript and approving it for publication was Xiwang Dong.

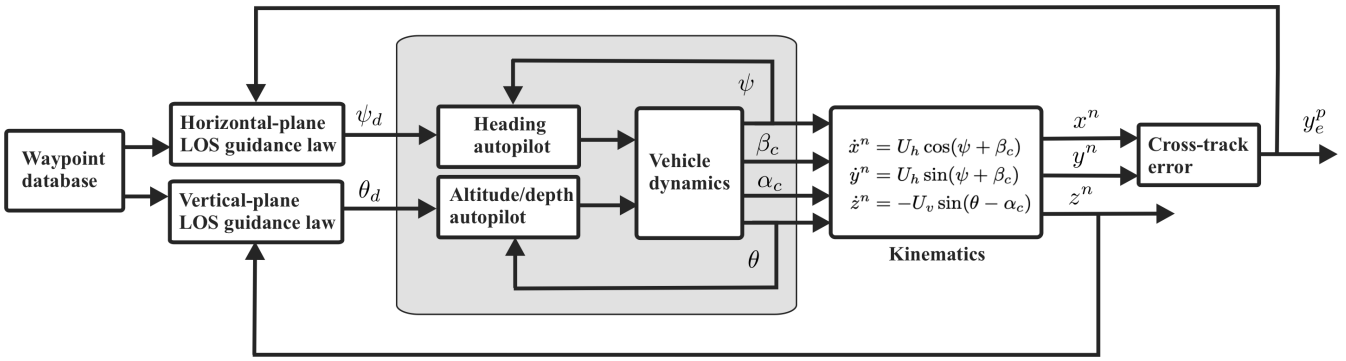

FIGURE 1. Feedback interconnection showing the LOS guidance laws (outer control loops) interacting with two commercial autopilots (inner control loops).

representation in guidance, navigation, and control applications. The main advantage of the kinematic amplitude-phase representation and its control inputs is simplicity when designing and analyzing the stability of vehicle LOS path-following control systems, as shown in Figure 1.

The rest of the paper is organized as follows. Section II presents the classical kinematic equations of a moving vehicle using Euler angle rotation matrices. Theorem 1 and Corollaries 1 and 2 summarize the amplitude-phase representation of the NED kinematic differential equations. In Section III, guidance laws for path following are presented, and the effectiveness of the guidance scheme is demonstrated by simulating an unmanned surface vehicle (USV) exposed to ocean currents. The concluding remarks are drawn in Section IV.

II. KINEMATICS

For marine craft and aircraft, the six different motion components in the BODY frame $\{b\}$ are conveniently defined as surge, sway, heave, roll, pitch and yaw. The NED reference frame is denoted by $\{n\}$.

A. NORTH-EAST-DOWN KINEMATIC DIFFERENTIAL EQUATIONS

Let $\boldsymbol{p}^n = [x^n, y^n, z^n]^\top$ denote the position vector expressed in $\{n\}$ and $\boldsymbol{v}^b = [u, v, w]^\top$ be the vehicle's linear velocity vector expressed in $\{b\}$. Consequently, the kinematic differential equations are given by [3]

$$\dot{\boldsymbol{p}}^n = \boldsymbol{R}_b^n \boldsymbol{v}^b \tag{1}$$

where $\dot{\boldsymbol{p}}^n = [\dot{x}^n, \dot{y}^n, \dot{z}^n]^\top$ denotes the positional rates and $\boldsymbol{R}_b^n$ is the rotation matrix *from* $\{b\}$ *to* $\{n\}$ defined by

$$\boldsymbol{R}_b^n = \begin{bmatrix} \mathrm{c}\psi\mathrm{c}\theta & -\mathrm{s}\psi\mathrm{c}\phi + \mathrm{c}\psi\mathrm{s}\theta\mathrm{s}\phi & \mathrm{s}\psi\mathrm{s}\phi + \mathrm{c}\psi\mathrm{c}\phi\mathrm{s}\theta \\ \mathrm{s}\psi\mathrm{c}\theta & \mathrm{c}\psi\mathrm{c}\phi + \mathrm{s}\phi\mathrm{s}\theta\mathrm{s}\psi & -\mathrm{c}\psi\mathrm{s}\phi + \mathrm{s}\theta\mathrm{s}\psi\mathrm{c}\phi \\ -\mathrm{s}\theta & \mathrm{c}\theta\mathrm{s}\phi & \mathrm{c}\theta\mathrm{c}\phi \end{bmatrix} \tag{2}$$

where $\mathrm{s}\cdot = \sin(\cdot)$ and $\mathrm{c}\cdot = \cos(\cdot)$. It is customary to describe $\boldsymbol{R}_b^n := \boldsymbol{R}_{z,\psi}\boldsymbol{R}_{y,\theta}\boldsymbol{R}_{x,\phi}$ by three *principal* rotations about the z, y and x axes (zyx convention) where ϕ, θ and ψ denote the Euler angles. Expanding (1) yields the positional rates in component form

$$\begin{aligned} \dot{x}^n &= u\cos(\psi)\cos(\theta) \\ &\quad + v\left(\cos(\psi)\sin(\theta)\sin(\phi) - \sin(\psi)\cos(\phi)\right) \\ &\quad + w\left(\sin(\psi)\sin(\phi) + \cos(\psi)\cos(\phi)\sin(\theta)\right) \end{aligned} \tag{3}$$

$$\begin{aligned} \dot{y}^n &= u\sin(\psi)\cos(\theta) \\ &\quad + v\left(\cos(\psi)\cos(\phi) + \sin(\phi)\sin(\theta)\sin(\psi)\right) \\ &\quad + w\left(\sin(\theta)\sin(\psi)\cos(\phi) - \cos(\psi)\sin(\phi)\right) \end{aligned} \tag{4}$$

$$\begin{aligned} \dot{z}^n &= -u\sin(\theta) \\ &\quad + v\cos(\theta)\sin(\phi) \\ &\quad + w\cos(\theta)\cos(\phi) \end{aligned} \tag{5}$$

B. AMPLITUDE-PHASE REPRESENTATION OF THE KINEMATIC DIFFERENTIAL EQUATIONS

This section presents a novel kinematic representation of the NED positional rates expressed by amplitudes and phase angles for coupled motions in 6 DOFs. As the rotation matrix representation (1), the proposed kinematic model gives equivalent NED positional rates for all combinations of the Euler angles and linear velocities. Previous work by [12] and [13] do not include the couplings between the *roll*, *pitch*, and *yaw* angles. Moreover, the roll dynamics has been neglected such that a 5-DOF simplified model could be derived under the assumption that $\phi \equiv 0$. In addition, a positive surge velocity $u > 0$ has been assumed. Theorem 1 below is the paper's main result, and it removes the previously discussed assumptions.

Theorem 1 (Kinematic Amplitude-Phase Representation): The kinematic differential equations (3)–(5) for positional rates can be expressed in 3-D amplitude-phase form according to

$$\dot{x}^n = U_h \cos(\psi + \beta_c) \tag{6}$$

$$\dot{y}^n = U_h \sin(\psi + \beta_c) \tag{7}$$

$$\dot{z}^n = -U_v \sin(\theta - \alpha_c) \tag{8}$$

The phase angles (α_c, β_c) and amplitudes (U_h, U_v) are

$$\alpha_c = \tan^{-1}\left(\frac{v\sin(\phi) + w\cos(\phi)}{u}\right) \tag{9}$$

$$\beta_c = \tan^{-1}\left(\frac{v\cos(\phi) - w\sin(\phi)}{U_v \cos(\theta - \alpha_c)}\right) \tag{10}$$

$$U_v = \sqrt{u^2 + (v\sin(\phi) + w\cos(\phi))^2} \tag{11}$$

$$U_h = \sqrt{(U_v\cos(\theta - \alpha_c))^2 + (v\cos(\phi) - w\sin(\phi))^2} \tag{12}$$

where the inverse tangent function,[1] $\tan^{-1}(y/x)$, is defined for all $x, y \in \mathbb{R}$. Note that $0 \leq U_h$ and $0 \leq |u| \leq U_v$.

Proof: See the Appendix.

For aircraft [2] and marine craft [3] moving with positive surge velocity $u > 0$, Corollaries 1 and 2 below can be applied.

Corollary 1 (6-DOF Model for Flying vehicles): A flying vehicle (under water and in air) with positive surge velocity $u > 0$ is a special case of Theorem 1 where

$$\dot{x}^n = U_h \cos(\psi + \beta_c) \tag{13}$$

$$\dot{y}^n = U_h \sin(\psi + \beta_c) \tag{14}$$

$$\dot{z}^n = -U_v \sin(\theta - \alpha_c) \tag{15}$$

$$\alpha_c = \tan^{-1}\left(\frac{v\sin(\phi) + w\cos(\phi)}{u}\right) \tag{16}$$

$$\beta_c = \tan^{-1}\left(\frac{v\cos(\phi) - w\sin(\phi)}{U_v\cos(\theta - \alpha_c)}\right) \tag{17}$$

$$U_v = u\sqrt{1 + \tan^2(\alpha_c)} \tag{18}$$

$$U_h = U_v\cos(\theta - \alpha_c)\sqrt{1 + \tan^2(\beta_c)} \tag{19}$$

for $0 < U_h$ and $0 < u \leq U_v$.

Corollary 2 (5-DOF Zero-Roll Model for Flying Vehicles): If $\phi \equiv 0$ and $u > 0$, Eqs. (13)–(19) reduce to

$$\alpha_c = \tan^{-1}\left(\frac{w}{u}\right) \tag{20}$$

$$\beta_c = \tan^{-1}\left(\frac{v}{U_v\cos(\theta - \alpha_c)}\right) \overset{\theta=0}{=} \tan^{-1}\left(\frac{v}{u}\right) \tag{21}$$

and

$$\dot{x}^n = U_h\cos(\chi) \tag{22}$$

$$\dot{y}^n = U_h\sin(\chi) \tag{23}$$

where

$$\chi := \psi + \beta_c \tag{24}$$

is the course over ground (COG) and

$$U_h = \sqrt{(U_v\cos(\theta - \alpha_c))^2 + v^2} \overset{\theta=0}{=} \sqrt{u^2 + v^2} \tag{25}$$

is the speed over ground (SOG). The phase angle β_c is recognized as the *crab angle*. A vehicle with nonzero β_c is said to *sideslip*. For the vertical motion (15) reduces to

$$\dot{z}^n = -U_v\sin(\gamma) \tag{26}$$

[1]The inverse tangent function, $\tan^{-1}(y/x)$, complies with the definition used by Matlab [15] and other programming languages where $x = 0$ implies that, $\tan^{-1}(y/0) = \text{sgn}(y)\frac{\pi}{2}$, where $\text{sgn}(y) = |y|/y$ is the signum function.

where $U_v = (u^2 + w^2)^{1/2}$ is the vertical-plane speed and

$$\gamma := \theta - \alpha_c \tag{27}$$

is the *flight-path angle*.

III. APPLICATIONS TO GUIDANCE AND CONTROL

The main advantage of the amplitude-phase representation (6)–(8) is that the pitch and yaw angles (θ, ψ) can be treated as control inputs for the cross- and vertical-track errors, respectively during path following, see Figure 1. Consider a 2-D straight-line segment in the horizontal plane specified by two waypoints (x_i^n, y_i^n) and (x_{i+1}^n, y_{i+1}^n) expressed in $\{n\}$. Let the origin of the path-tangential coordinate system $\{p\}$ be located at (x_i^n, y_i^n) such that the x_p-axis is pointing towards the next waypoint (x_{i+1}^n, y_{i+1}^n). The along- and cross-track errors (x_e^p, y_e^p) expressed in $\{p\}$ are obtained by rotating the North-East tracking errors an *azimuth angle* π_h about the z_n axis. This is mathematically equivalent to

$$\begin{bmatrix} x_e^p \\ y_e^p \end{bmatrix} = \boldsymbol{R}_{z,\pi_h}^\top \left(\begin{bmatrix} x^n \\ y^n \end{bmatrix} - \begin{bmatrix} x_i^n \\ y_i^n \end{bmatrix}\right) \tag{28}$$

where

$$\boldsymbol{R}_{z,\pi_h} = \begin{bmatrix} \cos(\pi_h) & -\sin(\pi_h) \\ \sin(\pi_h) & \cos(\pi_h) \end{bmatrix} \tag{29}$$

and

$$\pi_h = \tan^{-1}\left(\frac{y_{i+1}^n - y_i^n}{x_{i+1}^n - x_i^n}\right) \tag{30}$$

Time differentiation of (28) and Application of Corollary 1 yields

$$\dot{x}_e^p = U_h\cos(\psi + \beta_c - \pi_h) \tag{31}$$

$$\dot{y}_e^p = U_h\sin(\psi + \beta_c - \pi_h) \tag{32}$$

$$\dot{z}_e^n = -U_v\sin(\theta - \alpha_c) \tag{33}$$

Note that the vertical position error $z_e^n = z^n - z_d^n$, where z_d^n is the constant desired depth/altitude, is expressed in $\{n\}$. The path-following control objective is to regulate the cross-track error to zero $(y_e^p = 0)$ and the vertical position to the desired depth/altitude $(z^n = z_d^n)$. In addition, the surge velocity u can be used to control the speed U_h in (31) through (11)–(12). This is known as path tracking.

A. HORIZONTAL-PLANE LOS GUIDANCE LAW FOR PATH FOLLOWING

Path-following control systems for marine craft, aircraft, and small autonomous vehicles can be designed using LOS guidance laws. A surface vehicle is usually controlled using a heading or a course autopilot. The cross-track error can be regulated to zero $(y_e^p = 0)$ by designing a course autopilot such that $\chi = \chi_d$ where χ_d is the desired course angle. Since $\chi = \psi + \beta_c$, we can apply the proportional LOS guidance law

$$\chi_d = \pi_h - \tan^{-1}\left(\frac{1}{\Delta_h} y_e^p\right) \tag{34}$$

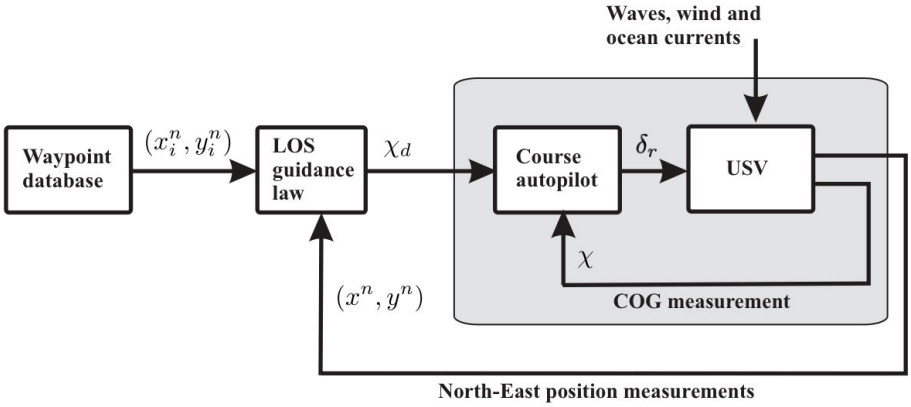

FIGURE 2. Course autopilot (inner control loop) and LOS guidance law (outer control loop) applied to a USV.

to (32) where $\Delta_h > 0$ is the user specified look-ahead distance. This gives the closed-loop dynamics

$$\dot{y}_e^p = U_h \sin\left(-\tan^{-1}\left(\frac{y_e^p}{\Delta_h}\right)\right) = -\frac{U_h}{\sqrt{\Delta_h^2 + (y_e^p)^2}}\, y_e^p \tag{35}$$

Consider the Lyapunov function candidate

$$V = \frac{1}{2}(y_e^p)^\top y_e^p \tag{36}$$

which after time differentiation and substitution of (35) becomes

$$\dot{V} = -\frac{U_h}{\sqrt{\Delta_h^2 + (y_e^p)^2}}\,(y_e^p)^2 \tag{37}$$

Lyapunov stability theory guarantees that the equilibrium point $y_e^p = 0$ of (35) is USGES if $U_h > 0$, see [4]. Alternatively, the vector field guidance law [16] can be applied. In some cases, it is advantageous to let the look-ahead distance Δ_h vary with time, e.g. by using optimization techniques [17] or the explicit formula by [18].

Next, consider the NTNU Autonaut shown in Figure 3, which is a long-endurance USV propelled by the motion of the waves [19]. The USV is controlled by a single rudder δ_r. The yaw angle transfer function is [3]

$$\frac{\psi}{\delta_r}(s) = \frac{K}{s(Ts+1)} \tag{38}$$

For the Autonaut, $K = 0.25\ \text{s}^{-1}$ and $T = 3.0$ s, see [21]. Hence, the North-East positions are obtained by integrating (22) and (23). Assume that the USV is exposed to stochastic ocean currents with initial speed $V_c = 0.2$ m/s and direction $\beta_{V_c} = 150$ deg. Hence, it follows that the ocean current velocities are $u_c = V_c \cos(\beta_{V_c})$ and $v_c = V_c \sin(\beta_{V_c})$, respectively. Furthermore, we assume that the USV moves at forward speed $U = 1.0$ m/s such that the velocities become

FIGURE 3. The NTNU Autonaut [20] is propelled by the motion of the waves. The vehicle's length is 4.6 m and the mass is 250 kg.

$u = U$ and $v = v_c$ during straight-line path following. Hence, we can compute the crab angle and course angle by

$$\beta_c = \tan^{-1}(v/u) = \tan^{-1}(v_c/U) \tag{39}$$

$$\chi = \psi + \beta_c \tag{40}$$

Since the USV dynamics is well damped, a proportional-integral (PI) controller is used to regulate the course angle

$$\delta_r = -K_p\, \text{ssa}(\chi - \chi_d) - K_i \int_0^t \text{ssa}(\chi - \chi_d)\text{d}\tau \tag{41}$$

where the numerical values $K_p = 1.25$ and $K_i = 0.02$ are based on [21]. The function, $\text{ssa}(x) = \text{mod}(x + \pi, 2\pi) - \pi$, is the *smallest-signed angle* confining the argument to the interval $[-\pi, \pi)$. Here $\text{mod}(\cdot)$ denotes the modulo operation or the signed remainder of a division. The closed-loop system is shown in Figure 2 where the inner control loop (41) regulates χ to χ_d. Note that the guidance law (34) represents the outer control loop. Consequently, the inner control loop can be replaced by a commercial autopilot system. The guidance

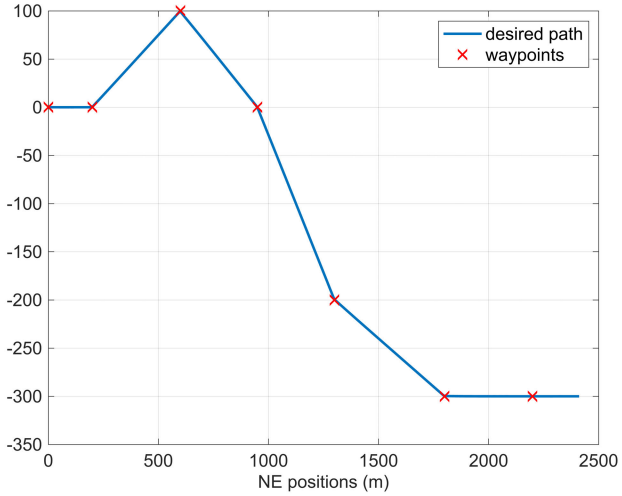

FIGURE 4. Desired waypoints and actual path during straight-line path following when a course autopilot controls the USV.

law (34) was implemented using a look-ahead distance $\Delta_h = 20$ m, and the sampling time was chosen as 20 Hz.

The desired vehicle path shown in Figure 4 consists of N straight-line segments specified by waypoints (x_i^n, y_i^n) where $i = 1, 2, \ldots, N$. Switching between the waypoints is an important feature when implementing straight-line path following control systems. The next waypoint (x_{i+1}^n, y_{i+1}^n) is selected based on whether or not the USV lies within a circle of acceptance with radius R around (x_{i+1}^n, y_{i+1}^n). In other words, if the USV's North-East positions (x^n, y^n) at time t satisfy [3]

$$(x_{i+1}^n - x^n)^2 + (y_{i+1}^n - y^n)^2 \leq R^2 \tag{42}$$

the next waypoint (x_{i+1}^n, y_{i+1}^n) is selected. The desired course angle and its true value are shown in Figure 5, confirming that $\chi \approx \chi_d$ during path following. At the same time, the magnitude of the cross-track error is less than 5 meters. The waypoint switching algorithm causes the steps. Hence, the accuracy will be much better, typically in the centimeter range, during straight-line path following.

The LOS guidance law (34) can also be implemented using a heading autopilot

$$\psi_d = \pi_h - \beta_c - \tan^{-1}\left(\frac{1}{\Delta_h} y_e^p\right) \tag{43}$$

which guarantees that the yaw angle $\psi \approx \psi_d$, where ψ_d is the desired yaw angle. This approach requires knowledge of the crab angle β_c. The crab angle is uncertain but nearly constant during the straight-line path following, see Figure 5. Hence, the preferred solution to this problem is to apply an integral LOS algorithm [22] to compensate for β_c. Alternatively, adaptive LOS guidance laws can be used to estimate β_c as shown by [14] and [23]. It is also possible to construct observers for estimation and compensation of β_c, see [24] and [25].

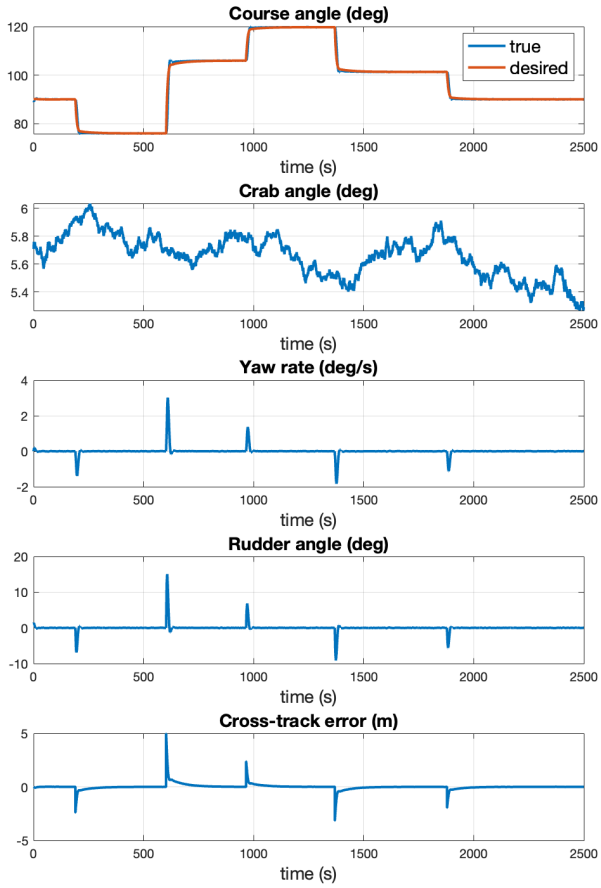

FIGURE 5. Course angle, crab angle, yaw rate, rudder angle and cross-track error versus time. A stochastic ocean current influences the crab angle. The switching of waypoints is observed as steps in the cross-track error.

B. VERTICAL-PLANE LOS GUIDANCE LAW FOR PATH FOLLOWING

LOS guidance laws can also be used to control the depth of an autonomous underwater vehicle (AUV) or the altitude of an aircraft by using θ in (33), alternatively the flight-path angle $\gamma = \theta - \alpha_c$, as the control input. Application of the proportional LOS guidance law

$$\gamma_d = \tan^{-1}\left(\frac{1}{\Delta_v} z_e^n\right) \tag{44}$$

to (33) where $\Delta_v > 0$ is the user-specified look-ahead distance, gives the closed-loop dynamics

$$\begin{aligned} \dot{z}^n &= -U_v \sin\left(\tan^{-1}\left(\frac{z_e^n}{\Delta_v}\right)\right) \\ &= -\frac{U_v}{\sqrt{\Delta_v^2 + (z_e^n)^2}} z^n \end{aligned} \tag{45}$$

This is based on the assumption that the inner control loop regulates γ to γ_d. Again Lyapunov stability theory guarantees that the origin $z^n = z_d^n$ of (45) is USGES if $U_v > 0$ [4]. Alternatively, a pitch angle command can be computed using

$\theta = \gamma - \alpha_c$. This requires knowledge of the signal α_c, which is uncertain but nearly constant during straight-line path following. However, integral LOS can be used to overcome this problem [3].

IV. CONCLUSION

This paper has presented a novel kinematic amplitude-phase representation of the North-East-Down (NED) positional rates, which can replace the classical Euler angle rotation matrix representation in guidance, navigation, and control applications. Several authors have discussed proportional line-of-sight (LOS) guidance laws for path following using approximate amplitude-phase models where couplings to the roll motion are neglected. The results in the paper generalize this to six degrees of freedom (DOFs) coupled motions by including the roll mode. The proposed kinematic model has three control inputs; the pitch and yaw angles (θ, ψ), and the surge velocity u. The main advantage of the kinematic amplitude-phase representation and its control inputs is simplicity when designing and analyzing the stability of vehicle LOS path-following control systems. A unmanned surface vehicle (USV) case study demonstrated how a path-following control system could be designed using the amplitude-phase representation.

APPENDIX.
PROOF OF THEOREM 1

Let $c_1 = A\cos(\varphi)$, $c_2 = A\sin(\varphi)$, $\varphi = \tan^{-1}(c_2/c_1)$ where $A = (c_1^2 + c_2^2)^{1/2}$. The inverse tangent function, $\tan^{-1}(y/x)$, is defined for all $x, y \in \mathbb{R}$. This complies with the definition used by Matlab [15] and other programming languages where $x = 0$ implies that, $\tan^{-1}(y/0) = \text{sgn}(y)\frac{\pi}{2}$, where $\text{sgn}(y) = |y|/y$ is the signum function. From this it follows that

$$\begin{aligned} y_1 &= c_1\sin(x) + c_2\cos(x) \\ &= A\sin(x)\cos(\varphi) + A\cos(x)\sin(\varphi) \\ &= A\sin(x+\varphi) \end{aligned} \tag{46}$$

$$\begin{aligned} y_2 &= c_1\cos(x) + c_2\sin(x) \\ &= A\cos(x)\cos(\varphi) + A\sin(x)\sin(\varphi) \\ &= A\cos(x-\varphi) \end{aligned} \tag{47}$$

Consider the kinematic differential equation (3)–(5) where the terms in ψ and θ can be collected according to

$$\begin{aligned} \dot{x}^n &= [-v\cos(\phi) + w\sin(\phi)]\sin(\psi) \\ &\quad + [u\cos(\theta) + v\sin(\theta)\sin(\phi) + w\sin(\theta)\cos(\phi)]\cos(\psi) \end{aligned} \tag{48}$$

$$\begin{aligned} \dot{y}^n &= [u\cos(\theta) + v\sin(\phi)\sin(\theta) + w\sin(\theta)\cos(\phi)]\sin(\psi) \\ &\quad + [v\cos(\phi) - w\sin(\phi)]\cos(\psi) \end{aligned} \tag{49}$$

$$\begin{aligned} \dot{z}^n &= -u\sin(\theta) \\ &\quad + [v\sin(\phi) + w\cos(\phi)]\cos(\theta) \end{aligned} \tag{50}$$

Next, we define $U_v = (u^2 + (v\sin(\phi) + w\cos(\phi))^2)^{1/2}$ and $\tan(\alpha_c) = (v\sin(\phi) + w\cos(\phi))/u$ such that the common terms in (48) and (49) can be rewritten as

$$\begin{aligned} &u\cos(\theta) + (v\sin(\phi) + w\cos(\phi))\sin(\theta) \\ &\quad = U_v\cos(\theta - \alpha_c) \end{aligned} \tag{51}$$

Consequently, (48)–(50) can be expressed by

$$\begin{aligned} \dot{x}^n &= [-v\cos(\phi) + w\sin(\phi)]\sin(\psi) \\ &\quad + U_v\cos(\theta - \alpha)\cos(\psi) \end{aligned} \tag{52}$$

$$\begin{aligned} \dot{y}^n &= U_v\cos(\theta - \alpha)\sin(\psi) \\ &\quad + [v\cos(\phi) - w\sin(\phi)]\cos(\psi) \end{aligned} \tag{53}$$

$$\begin{aligned} \dot{z}^n &= -u\sin(\theta) \\ &\quad + [v\sin(\phi) + w\cos(\phi)]\cos(\theta) \end{aligned} \tag{54}$$

Application of (46)–(47) to (52)–(54) prove (6)–(8) where

$$\alpha_c = \tan^{-1}\left(\frac{v\sin(\phi) + w\cos(\phi)}{u}\right) \tag{55}$$

$$\beta_c = \tan^{-1}\left(\frac{v\cos(\phi) - w\sin(\phi)}{U_v\cos(\theta - \alpha_c)}\right) \tag{56}$$

and

$$U_v = \sqrt{u^2 + (v\sin(\phi) + w\cos(\phi))^2} \tag{57}$$

$$U_h = \sqrt{(U_v\cos(\theta - \alpha_c))^2 + (v\cos(\phi) - w\sin(\phi))^2} \tag{58}$$

If $u \equiv 0$ and/or $U_v\cos(\theta - \alpha_c) \equiv 0$, the inverse tangent function is defined such that (55) and (56) are equal the limiting values $\alpha_c = \pm\pi/2$ and $\beta_c = \pm\pi/2$, respectively. This guarantees that (55)–(58) are well defined for all surge velocities u (Theorem 1). For flying vehicles, $u > 0$, Equation (57)–(58) can be further simplified as

$$U_v = u\sqrt{1 + \tan^2(\alpha_c)} \tag{59}$$

$$U_h = U_v\cos(\theta - \alpha_c)\sqrt{1 + \tan^2(\beta_c)} \tag{60}$$

which proofs Corollary 1.

REFERENCES

[1] M. Breivik and T. I. Fossen, "Principles of guidance-based path following in 2-D and 3-D," in *Proc. IEEE Conf. Decis. Control, Eur. Control Conf.*, Seville, Spain, Dec. 2005, pp. 627–634.

[2] R. W. Beard and T. W. McLain, *Small Unmanned Aircraft: Theory and Practice*. Princeton, NJ, USA: Princeton Univ. Press, 2012.

[3] T. I. Fossen, *Handbook of Marine Craft Hydrodynamics and Motion Control*, 2nd ed. Chichester, U.K.: Wiley, 2021.

[4] T. I. Fossen and K. Y. Pettersen, "On uniform semiglobal exponential stability (USGES) of proportional line-of-sight guidance laws," *Automatica*, vol. 50, no. 11, pp. 2912–2917, Nov. 2014.

[5] A. J. Healey and D. Lienard, "Multivariable sliding mode control for autonomous diving and steering of unmanned underwater vehicles," *IEEE J. Ocean. Eng.*, vol. 18, no. 3, pp. 327–339, Jul. 1993.

[6] K. Y. Pettersen and E. Lefeber, "Way-point tracking control of ships," in *Proc. IEEE Conf. Decis. Control*, Orlando, FL, USA, Feb. 2001, pp. 940–945.

[7] E. Borhaug and K. Y. Pettersen, "Cross-track control for underactuated autonomous vehicles," in *Proc. 44th IEEE Conf. Decis. Control*, Seville, Spain, Dec. 2005, pp. 602–608.

[8] E. Fredriksen and K. Y. Pettersen, "Global κ-exponential waypoint maneuvering of ships: Theory and experiments," *Automatica*, vol. 42, no. 4, pp. 677–687, 2006.

[9] D. R. Nelson, D. B. Barber, T. W. McLain, and R. W. Beard, "Vector field path following for miniature air vehicles," *IEEE Trans. Robot.*, vol. 23, no. 3, pp. 519–529, Jun. 2007.
[10] S. Park, J. Deyst, and J. P. How, "Performance and Lyapunov stability of a nonlinear path following guidance method," *J. Guid. Control Dyn.*, vol. 30, no. 6, pp. 1718–1728, 2007.
[11] M. Breivik and T. I. Fossen, "Guidance laws for autonomous underwater vehicles," in *Intelligent Underwater Vehicles*, A. V. Inzartsev, Ed. Vienna, Austria: I-Tech Education, 2009, pp. 51–76.
[12] A. M. Lekkas and T. I. Fossen, "Line-of-sight guidance for path following of marine vehicles," in *Advanced in Marine Robotics*, O. Gal, Ed. London, U.K.: LAP LAMBERT Academic, 2013, pp. 63–92.
[13] W. Caharija, "Integral line-of-sight guidance and control of underactuated marine vehicles," Ph.D. dissertation, Dept. Eng. Cybern., Norwegian Univ. Sci. Technol., Trondheim, Norway, 2014.
[14] T. I. Fossen, K. Y. Pettersen, and R. Galeazzi, "Line-of-sight path following for Dubins paths with adaptive sideslip compensation of drift forces," *IEEE Trans. Control Syst. Technol.*, vol. 23, no. 2, pp. 820–827, Mar. 2015.
[15] *The MathWorks Inc.*, MATLAB, Natick, MA, USA, 2022.
[16] H. Xu, T. I. Fossen, and C. Guedes Soares, "Uniformly semiglobally exponential stability of vector field guidance law and autopilot for path-following," *Eur. J. Control*, vol. 53, pp. 88–97, May 2020.
[17] A. Pavlov, H. Nordahl, and M. Breivik, "MPC-based optimal path following for underactuated vessels," in *Proc. IFAC Conf. Maneouvring Control Mar. Craft*, Sao Paulo, Brazil, 2009, 340–345.
[18] A. M. Lekkas and T. I. Fossen, "A time-varying lookahead distance guidance law for path following," *IFAC Proc. Volumes*, vol. 45, no. 27, pp. 398–403, 2012.
[19] P. Johnston and M. Poole, "Marine surveillance capabilities of the autonaut wave-propelled unmanned surface vessel (USV)," in *Proc. OCEANS*, Aberdeen, U.K., 2017, pp. 1–46.
[20] Norwegian University of Science and Technology. *AutoNaut Documentation Wiki*. Accessed: Jan. 2023. [Online]. Available: https://autonaut.itk.ntnu.no/doku.php
[21] A. Dallolio, H. Øveraas, J. A. Alfredsen, T. I. Fossen, and T. A. Johansen, "Design and validation of a course control system for a wave-propelled unmanned surface vehicle," *Field Robot.*, vol. 2, pp. 774–806, 2022. [Online]. Available: https://fieldrobotics.net/Field_Robotics/Volume_2.html
[22] E. Borhaug, A. Pavlov, and K. Y. Pettersen, "Integral LOS control for path following of underactuated marine surface vessels in the presence of constant ocean currents," in *Proc. 47th IEEE Conf. Decis. Control*, Cancun, Mexico, Dec. 2008, pp. 4984–4991.
[23] T. I. Fossen and A. M. Lekkas, "Direct and indirect adaptive integral line-of-sight path-following controllers for marine craft exposed to ocean currents," *Int. J. Adapt. Control*, vol. 31, no. 4, pp. 445–463, Mar. 2015.
[24] L. Liu, D. Wang, Z. Peng, and H. Wang, "Predictor-based LOS guidance law for path following of underactuated marine surface vehicles with sideslip compensation," *Ocean Eng.*, vol. 124, pp. 340–348, Sep. 2016.
[25] L. Liu, D. Wang, and Z. Peng, "ESO-based line-of-sight guidance law for path following of underactuated marine surface vehicles with exact sideslip compensation," *IEEE J. Ocean. Eng.*, vol. 42, no. 2, pp. 477–487, Apr. 2017.

THOR I. FOSSEN (Fellow, IEEE) received the M.Sc. degree in marine technology and the Ph.D. degree in engineering cybernetics from the Norwegian University of Science and Technology (NTNU), Trondheim, in 1987 and 1991, respectively.

He is one of the co-founders and the former Vice President of the Research and Development at Marine Cybernetics AS, which was acquired by DNV, in 2012. He was the Co-Founder of ScoutDI AS, in 2017. He is currently a Professor of guidance, navigation, and control. He is also a Naval Architect and a Cyberneticist. He has authored six textbooks and editorials, including the *Handbook of Marine Craft Hydrodynamics and Motion Control* published by John Wiley & Sons Ltd. His research interests include guidance systems, inertial navigation systems, nonlinear control and observer theory, vehicle dynamics, hydrodynamics, autopilots, marine craft, and unmanned vehicles.

Dr. Fossen has been elected to the Norwegian Academy of Technological Sciences, in 1998, and the Norwegian Academy of Science and Letters, in 2022. He received the Automatica Prize Paper Award, in 2002, and the Arch T. Colwell Merit Award, in 2008, from the SAE World Congress.